



## RESEARCH LETTER

10.1002/2017GL073377

## Special Section:

Early Results: Juno at Jupiter

## Key Points:

- Jupiter's aurora and the solar wind have a complex relationship
- The single solar wind structure that correlated with an auroral brightening event was a CIR
- Auroral brightening events which are not related to solar wind conditions have a similar time evolution

## Supporting Information:

- Supporting Information S1
- Movie S1

## Correspondence to:

G. R. Gladstone,  
rgladstone@swri.edu

## Citation:

Gladstone, G. R., et al. (2017), Juno-UVS approach observations of Jupiter's auroras, *Geophys. Res. Lett.*, *44*, 7668–7675, doi:10.1002/2017GL073377.

Received 7 MAR 2017

Accepted 18 APR 2017

Published online 4 AUG 2017

©2017. The Authors.

This is an open access article under the terms of the Creative Commons Attribution-NonCommercial-NoDerivs License, which permits use and distribution in any medium, provided the original work is properly cited, the use is non-commercial and no modifications or adaptations are made.

## Juno-UVS approach observations of Jupiter's auroras

G. R. Gladstone<sup>1,2</sup> , M. H. Versteeg<sup>1</sup> , T. K. Greathouse<sup>1</sup> , V. Hue<sup>1</sup> , M. W. Davis<sup>1</sup> , J.-C. Gérard<sup>3</sup> , D. C. Grodent<sup>3</sup> , B. Bonfond<sup>3</sup> , J. D. Nichols<sup>4</sup> , R. J. Wilson<sup>5</sup> , G. B. Hospodarsky<sup>6</sup> , S. J. Bolton<sup>1</sup> , S. M. Levin<sup>7</sup> , J. E. P. Connerney<sup>8</sup> , A. Adriani<sup>9</sup> , W. S. Kurth<sup>6</sup> , B. H. Mauk<sup>10</sup> , P. Valek<sup>1</sup> , D. J. McComas<sup>11</sup> , G. S. Orton<sup>7</sup> , and F. Bagenal<sup>5</sup>

<sup>1</sup>Southwest Research Institute, San Antonio, Texas, USA, <sup>2</sup>Department of Physics and Astronomy, University of Texas at San Antonio, San Antonio, Texas, USA, <sup>3</sup>STAR Institute, LPAP, Université de Liège, Liège, Belgium, <sup>4</sup>Department of Physics and Astronomy, University of Leicester, Leicester, UK, <sup>5</sup>Laboratory for Atmospheric and Space Physics, University of Colorado Boulder, Boulder, Colorado, USA, <sup>6</sup>Department of Physics and Astronomy, University of Iowa, Iowa City, Iowa, USA, <sup>7</sup>Jet Propulsion Laboratory, Pasadena, California, USA, <sup>8</sup>NASA Goddard Space Flight Center, Greenbelt, Maryland, USA, <sup>9</sup>Istituto di Astrofisica e Planetologia Spaziali, Rome, Italy, <sup>10</sup>The Johns Hopkins University Applied Physics Laboratory, Laurel, Maryland, USA, <sup>11</sup>Office of the VP for PPPL and Department of Astrophysical Sciences, Princeton University, Princeton, New Jersey, USA

**Abstract** Juno ultraviolet spectrograph (UVS) observations of Jupiter's aurora obtained during approach are presented. Prior to the bow shock crossing on 24 June 2016, the Juno approach provided a rare opportunity to correlate local solar wind conditions with Jovian auroral emissions. Some of Jupiter's auroral emissions are expected to be controlled or modified by local solar wind conditions. Here we compare synoptic Juno-UVS observations of Jupiter's auroral emissions, acquired during 3–29 June 2016, with in situ solar wind observations, and related Jupiter observations from Earth. Four large auroral brightening events are evident in the synoptic data, in which the total emitted auroral power increases by a factor of 3–4 for a few hours. Only one of these brightening events correlates well with large transient increases in solar wind ram pressure. The brightening events which are not associated with the solar wind generally have a risetime of ~2 h and a decay time of ~5 h.

**Plain Language Summary** Juno ultraviolet spectrograph (UVS) observations of Jupiter's aurora obtained during approach are presented. Jupiter's auroras are thought to be controlled in part by the solar wind, a stream of charged particles flowing outward from the Sun. The Juno approach was a rare opportunity to compare solar wind conditions near Jupiter with the Jovian ultraviolet aurora, using observations made during June 2016. Although Jupiter's aurora is always present, four brightening events were seen in the data, in which the total auroral power increased to several times the typical level for a few hours. Only one of these brightening events appears well connected with solar wind activity. The brightening events which are not associated with the solar wind all increase in brightness in about 2 h and then dim back down again in about another 5 h.

## 1. Introduction

Jupiter's far ultraviolet auroras have been observed by spacecraft and Earth-orbiting satellites for several decades, and our understanding of these emissions has evolved considerably [e.g., *Broadfoot et al.*, 1979; *Prangé et al.*, 1996; *Bhardwaj and Gladstone*, 2000; *Ajello et al.*, 2001; *Clarke et al.*, 2004, 2009; *Pryor et al.*, 2005; *Nichols et al.*, 2009; *Grodent*, 2015; *Tao et al.*, 2015a, 2015b; *Badman et al.*, 2015]. There are four primary types or regions of Jovian aurora: (1) the main emissions, driven by the breakdown of corotation in the plasma of the middle magnetosphere; (2) polar emissions that may be associated with reconnection regions near the dayside magnetopause or in the magnetotail; (3) emissions associated with the magnetic footprints of the Galilean satellites; and (4) low-latitude emissions, including blobs attributed to plasma injections and diffuse emissions attributed to pitch angle diffusion of energetic electrons. One of the primary science goals of the Juno mission is to explore and learn about Jupiter's polar magnetosphere [*Bagenal et al.*, 2014]. In particular, using in situ and remote sensing observations, we hope to discover where and how precipitating auroral particles are energized; what processes result in transient auroras, such as the polar emissions; and, regarding the present study, how the auroras are affected by changes in the solar wind near Jupiter.

NASA's Juno mission arrived at Jupiter on 5 July 2016 and is currently in an ~53 day polar orbit with an apojuve at ~112 Jupiter radii ( $R_J$ ) and a perijuve at ~1.05  $R_J$  (roughly 4000 km above the cloud tops). A primary goal of Juno ultraviolet spectrograph (UVS) is to remotely sense Jupiter's auroral morphology and brightness

to provide context for in situ measurements by Juno's particle and field instruments. During the 6 month approach phase prior to Jupiter Orbit Insertion (JOI), many Juno instruments were used to make regular remote observations of Jupiter and in situ measurements of the local solar wind. During this phase, Juno-UVS observed Jupiter for about 10 h on 25 January, 17 February, 16 March, 11 April, and 10 May 2016. These early Jupiter approach data will not be further discussed here. Juno-UVS began a long synoptic observation of Jupiter's auroral emissions at 02:30:00 UT on 3 June 2016 and completed these observations at 23:59:24 on 29 June 2016. While synoptic observations of Jupiter's auroral emissions have been acquired previously, most notably by Galileo and Cassini during the Cassini flyby [e.g., Gurnett *et al.*, 2002; Pryor *et al.*, 2005], by Hubble Space Telescope (HST) Advanced Camera for Surveys during the New Horizons flyby in 2007 [e.g., Clarke *et al.*, 2009; Nichols *et al.*, 2009], and more recently by Hisaki in 2015 [e.g., Tao *et al.*, 2015a, 2015b; Kita *et al.*, 2016; Kimura *et al.*, 2016] and HST support of Juno [Nichols *et al.*, 2017], the Juno-UVS data provide a considerable addition to these earlier studies, due to their unique vantage point above the dawn terminator and the availability of simultaneous solar wind parameters obtained by the Jovian Auroral Distributions Experiment (JADE) in situ plasma instrument on Juno. In the following sections we (1) briefly review Juno-UVS and the circumstances of the June 2016 approach observations, (2) present examples of the acquired data and the derived emitted UV auroral power, (3) examine time dependence for several brightening events, and (4) summarize how these results compare with previous studies. For a look at initial Juno-UVS data for the first Juno science peri-jove on 27 August 2016, interested readers are referred to Bonfond *et al.* [2017] and Connerney *et al.* [2017].

## 2. Observations

Juno-UVS is an imaging spectrograph with a band pass of  $70 < \lambda < 205$  nm, which includes all important ultraviolet (UV) emissions (primarily the Lyman and Werner bands of  $H_2$  and the Lyman series of H) produced in Jupiter's auroras [Gladstone *et al.*, 2014]. The Juno-UVS instrument telescope has a  $4 \times 4$  cm<sup>2</sup> input aperture and uses an off-axis parabolic primary mirror. A flat scan mirror situated near the entrance of the telescope is used to observe at up to  $\pm 30^\circ$  perpendicular to the Juno spin plane, with positive angles defined as being toward the spin axis. During the June 2016 approach observations, the Juno spin axis was pointed near Earth, and the Earth-Juno-Jupiter angle ranged from  $103.4^\circ$  to  $101.5^\circ$ . Light from the primary mirror is focused onto the spectrograph entrance slit, which has a "dog-bone" shape  $7.5^\circ$  long, in three sections of  $0.2^\circ \times 2.5^\circ$ ,  $0.025^\circ \times 2.0^\circ$ , and  $0.2^\circ \times 2.5^\circ$  width (as projected onto the sky). During the synoptic observations discussed here, the angular diameter of Jupiter ranged from  $0.38^\circ$  to  $1.56^\circ$ , allowing Jupiter to be centered in one of the  $0.2^\circ \times 2.5^\circ$  "wide" sections throughout; this enabled masking of the remaining slit to reduce the total data volume produced. Light entering the slit is dispersed by a toroidal grating which focuses UV light onto a curved microchannel plate (MCP) cross delay line detector, which has a solar-blind CsI photocathode. The filled wide-slit spectral resolution is  $\sim 2.2$  nm [Greathouse *et al.*, 2013]. Tantalum shielding surrounds the spectrograph assembly to protect the detector and its electronics from high-energy particles (mostly electrons trapped in Jupiter's radiation belts and magnetodisk). The remaining Juno-UVS electronics, including redundant low-voltage and high-voltage power supplies, command and data handling electronics, heater/actuator electronics, scan mirror electronics, and event processing electronics, are located in the spacecraft vault.

Although the vantage point of Juno above the dawn terminator varied slowly (the sub-spacecraft latitude increased from  $8.9^\circ$ N to  $13.2^\circ$ N) during the June 2016 approach observations, the range to Jupiter dropped by a factor of 4.1, from  $302.0$  to  $73.4 R_J$ . Figure 1 shows the location of Juno relative to Jupiter during this period, as seen from Earth. Because Juno is a spinning spacecraft, the Juno-UVS detector is operated in "pixel list" mode, in which individual photon events are recorded by their  $x$  (wavelength) and  $y$  (position along the slit) locations on the MCP detector, with "time hacks" inserted into the data stream at 1–512 ms intervals to provide timing information. When the scan mirror is pointed in the Juno spin plane, the Juno-UVS slit is oriented perpendicular to the spin motion, allowing 2-D images to be constructed using the photon's position along the slit and the spin phase of the spacecraft at the nearest time hack to the photon event as the spatial dimensions. When the scan mirror is pointed off the spin plane by an angle  $\Theta$ , the slit is tilted by an equal angle  $\Theta$  and the time a point source remains in the wide slit during one spin varies as  $t_{\text{SPIN}} (d_{\text{SW}}/360)/\cos^2\Theta \sim 16.7 \text{ ms}/\cos^2\Theta$  for the  $0.2^\circ$ -wide slit, where  $t_{\text{SPIN}}$  is the Juno spin period and  $d_{\text{SW}}$  is the slit width. For the June approach data, the time hack interval was set at 8 ms; at Juno's nominal 30 s spin period, this corresponds to an angle on the sky of  $0.096^\circ$ , about half the  $0.2^\circ$  slit width. Juno-UVS data are thus

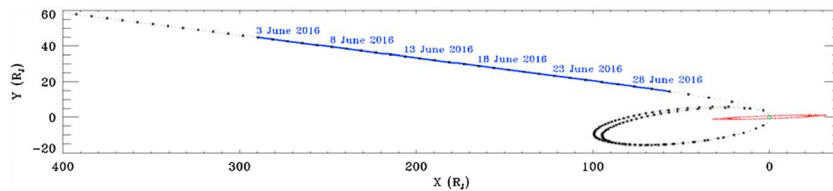


**Figure 1.** The location of the Juno spacecraft during approach as seen from Earth, with x and y axes parallel to ecliptic longitude and latitude, respectively, in units of Jupiter radii (the dots mark every 6 h; the asterisks mark each day). The nearly contiguous Juno-UVS synoptic auroral observations from 3 to 29 June 2016 are indicated in blue, while Jupiter is outlined in green, and the orbit of Callisto is shown in red. During the synoptic observations, the spacecraft range to Jupiter center dropped from 302.0 to 73.4  $R_J$ , so that the angular diameter of Jupiter as seen from Juno increased from 0.38° to 1.56°.

effectively stored on the spacecraft and telemetered to Earth as a list of photon events, with wavelength and spatial location on the sky, which are then assembled into spectral images. In order to meet spacecraft telemetry limits, about 40 min of data were collected for each elapsed hour. For the June approach data, it was found that reasonable signal-to-noise ratio was obtained by coadding the photon events into 1 h frames (i.e., ~120 spins), amounting to an exposure time of 1.41 to 1.39 s per frame for the approach  $\Theta$  values of 13.4° to 11.5°.

The ~27 days of Juno-UVS observations were occasionally interrupted to repoint the Juno spacecraft antenna toward Earth. The repointing procedure usually took about 10 h to complete and resulted in nine data gaps as listed in Table 1. Added together, these data gaps total 77.59 h missing out of the total contiguous observation period of 645.49 h, or 12.0% of 65.0 consecutive rotations of Jupiter.

For each of the ~645 1 h frames of reduced data, images of total auroral brightness over a  $2^\circ \times 2^\circ$  region of the sky centered on Jupiter were created, integrating wavelengths from 70 to 119 nm plus 123–162 nm (the region around Lyman alpha at 121.6 nm was masked to reduce data volume) and converting from counts/s to kiloRayleighs/nm using the effective area determined through stellar calibrations acquired during Juno’s cruise phase [Greathouse *et al.*, 2013], scaled downward by a factor of ~2.1 to account for more thorough stellar calibrations since that preliminary result. This spectral range encompasses the  $H_2$  bands (Lyman, Werner, and Rydberg) and H Lyman series lines which comprise nearly all of Jupiter’s UV auroral emissions, while excluding most of the reflected sunlight at the long wavelength end of the Juno-UVS band pass. In addition to the total brightness, color ratio images were also created using brightness images of the  $H_2$  Lyman band emissions in the wavelength range of 155–162 nm divided by the brightness images of the  $H_2$  Lyman and Werner band emissions in the wavelength range of 123–130 nm. The color ratio [e.g., *Yung et al.*, 1982; *Gérard et al.*, 2014] is diagnostic of the energy of the precipitating particles (e.g., magnetospheric electrons), with larger values indicating more energetic particles, since these penetrate more deeply into Jupiter’s atmosphere and result in photons that are preferentially absorbed by methane at wavelengths <140 nm.

**Table 1.** Data Gaps<sup>a</sup>

Gap #	Start Day of June 2016	Start UTC (hh:mm:ss)	End Day of June 2016	End UTC (hh:mm:ss)	Gap Length (hh:mm:ss)
1	4	08:29:44	4	18:30:00	10:00:16
2	9	18:29:24	10	04:30:00	10:00:36
3	13	22:29:24	14	08:30:00	10:00:36
4	15	14:29:24	16	00:30:00	10:00:36
5	17	16:29:24	18	02:30:00	10:00:36
6	21	00:29:24	21	10:30:00	10:00:36
7	24	08:29:24	24	13:30:00	05:00:36
8	25	14:29:24	26	00:30:00	10:00:36
9	27	11:29:24	27	14:00:00	02:30:36
Total					77:35:04

<sup>a</sup>Due to repointings of the Juno antenna to Earth there were several gaps during the synoptic auroral observations made during 3–29 June 2016.

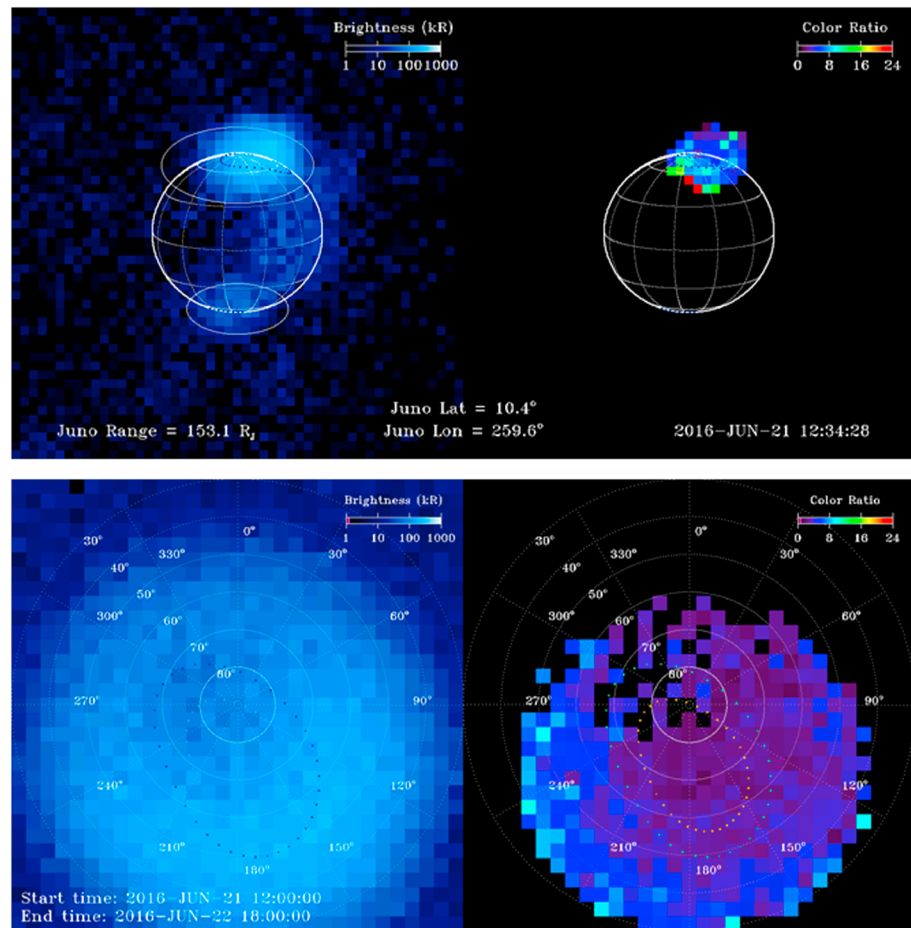


**Figure 2.** (a) (left) Juno-UVS brightness image and (right) corresponding color ratio image of Jupiter, for 1 h of elapsed time ( $\sim 1.3$  s integrated time) starting at 12:34:28 spacecraft UT on 21 June 2016. The Juno range and subspacecraft system III longitude and latitude are indicated, along with nominal  $L = 6$  and  $L = 30$  auroral ovals. The larger and smaller white ovals at the north and south poles in the brightness image indicate the regions included in estimating the northern and southern emitted auroral power, respectively. Brightness (and color ratio) pixels have an angular size of  $0.04^\circ \times 0.04^\circ$ , which considerably oversamples the instrument spatial point-spread function of along slit full width at half maximum FWHM  $\sim 0.20^\circ$ , cross slit FWHM  $\sim 0.25^\circ$  [Greathouse *et al.*, 2013]. The color ratios are only shown for pixels where the brightness both exceeds 80 kR and is larger than 25% of the peak brightness. See supporting information for an animation of the entire observation period. (b) (left) Juno-UVS brightness map and (right) corresponding color ratio map of Jupiter, for 30 h of elapsed time ( $\sim 38$  s integrated time) starting at 12:00:00 spacecraft UT on 21 June 2016. The  $L = 6$  and  $L = 30$  auroral ovals are indicated. The color ratios are only shown for pixels where the brightness both exceeds 80 kR and is larger than 25% of the peak brightness.

Figure 2a shows an example of the brightness and color ratio images created for the June approach data, for the 1 h period starting at 12:34:28 UT on 21 June 2016. This period is during the beginning of the last of four northern aurora brightening events seen in the synoptic data. The total exposure time of the image is only  $\sim 1.3$  s, due to the small width of the Juno-UVS slit and duty cycle of the spinning spacecraft. The color ratio, only shown when the brightness of a given pixel is  $>80$  kR (to exclude nonauroral emissions) and  $>25\%$  as bright as the brightest pixel in the image (to highlight the best signal-to-noise ratio observations), is not generally correlated with the brightest regions of the aurora but very often largest along the equatorward boundary and toward the nightside of Jupiter. This behavior does not seem to depend strongly on the activity level of the aurora. This is a new result and may indicate a source of high-energy, low-latitude precipitating particles from the anti-Sunward direction (e.g., nightside plasma injections), which is particularly well-observed from the Juno approach view from above the dawn terminator. Similar behavior has been seen in earlier HST observations (e.g., feature B in Gérard *et al.* [2014, Figure 2]) and is also notable in the Juno-UVS results from the first science perijove [Connerney *et al.*, 2017]. Figure 2b shows that north polar

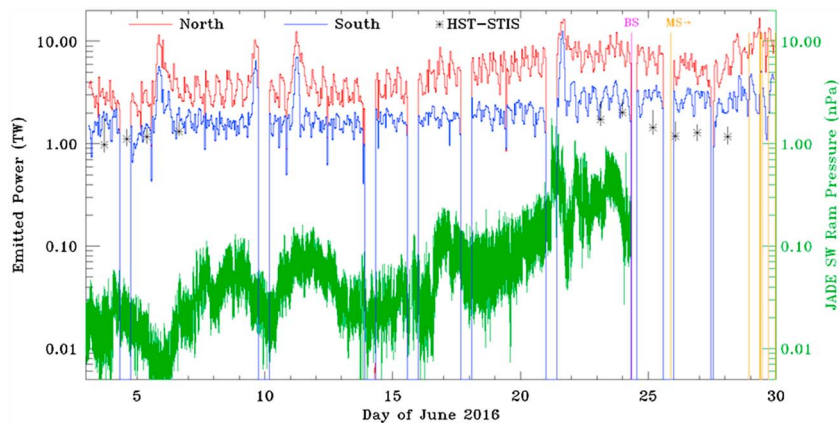


**Figure 3.** Estimated total emitted power observed with Juno-UVS from Jupiter's northern aurora (red) and more poorly observed southern aurora (blue), averaged over 1 h intervals during ~64 contiguous rotations of Jupiter over 3–30 June 2016 (day of year 155–182). Occasional data dropouts of ~10 h were due to periodic repointing of Juno's antenna toward Earth. The total solar wind ram pressure measured by JADE is shown for comparison (green, with the vertical spread indicating  $\pm 1\sigma$  errors), along with HST-STIS estimates of total emitted power from the northern aurora (black asterisks). The single approach-phase bow shock crossing on 24 June 2016 at 08:16 UT is indicated by a vertical purple line and subsequent magnetopause crossings by vertical orange lines.

maps of brightness and color ratio, using Juno-UVS data, obtained a 30 h period from 21 June 2016 at 12:00 UT until 22 June 2016 at 18:00 UT. Although the mapping at such large distances has poor spatial resolution, the color ratio map shows an interesting equatorial enhancement at system III longitudes in the  $120^{\circ}$ – $300^{\circ}$  range. An animation of the entire data set, from which Figure 2 is taken, is provided in the supporting information.

The spatial resolution is quite poor at the large distance of Juno from Jupiter during approach (i.e., much worse than provided by HST [e.g., Gérard *et al.*, 2014; Gustin *et al.*, 2016; Grodent, 2015]), but the integrated emission (indicated in Figure 2 by the ellipses centered on each pole) provides a useful measure of the total emitted auroral power from the northern and southern auroras. The total flux at the spacecraft received from the northern and southern auroras in the 70–119 nm plus 123–162 nm band pass is scaled by a factor of 1.2 to correct for the fraction of  $H_2$  band and Lyman  $\alpha$  emission missing in the data (using a high-resolution model  $H_2$  spectrum provided by J. Gustin (personal communication, 2008)). In order to estimate the emitted auroral power for the regions of the northern and southern auroras which are out of view of the spacecraft, we scale the measured emitted power by the geometric mean of the ratio of projected total lengths to projected observable lengths of the VIP4 model  $L = 6$  and  $L = 30$  ovals (similar to the correction applied by Nichols *et al.* [2009]). This procedure is imperfect at removing an obvious 10 h modulation in the total emitted power, but it does reduce it considerably.

### 3. Results

The total emitted power from the northern and more poorly viewed southern auroras during 3–29 June 2016 are shown in Figure 3, along with the JADE-determined solar wind ram pressure [McComas *et al.*, 2013], and some overlapping emitted auroral powers from HST Space Telescope Imaging Spectrograph (HST-STIS) observations [Nichols *et al.*, 2017]. The JADE data are derived from 1-D fits to low-rate time-of-flight measurements of the density and speed of solar wind protons and alpha particles obtained from 15 May 2016 until 24 June 2016. Although the  $3\sigma$  errors due to counting statistics are  $<1\%$  for the Juno-UVS total emitted auroral powers plotted in Figure 3, and thus, the observed relative variations are accurate, the absolute errors are currently estimated to be no less than ~50%, based on the preliminary calibration and assumptions made about the unseen auroral emissions. Although the correction (discussed at the end of the previous section) does help to reduce the visibility-induced 10 h periodicity in the total emitted power estimates, it is certainly not perfect. The power estimates with the best view (and least applied corrections) are those near the peaks of the remaining 10 h periodicity; i.e., the largest total emitted powers are likely the most accurate. The baseline total emitted northern auroral power is ~3 TW, while the baseline total emitted southern auroral

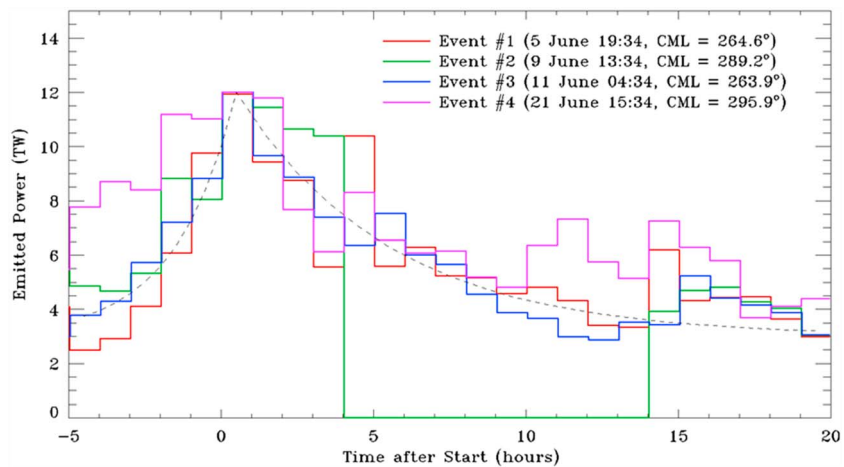


**Figure 4.** Profiles of total emitted power from Jupiter's northern aurora observed by Juno-UVS, averaged over 1 h intervals during four major brightening events. The events each had peak emitted powers in the 9–15 TW range but have been normalized to a peak of 12 TW in this plot and overlaid by start time in order to compare their time dependencies. For comparison, the dashed black line shows an exponential increase from the baseline emitted power of 3 TW up to a peak of 12 TW (with a  $1/e$  risetime of 2 h) and a decay back to the baseline emitted power (with a  $1/e$  dimming time of 5 h).

power is  $\sim 2$  TW, although the view of the southern aurora is quite foreshortened from Juno's location. The total emitted power is roughly bimodal, with an excited value about 3–4 times larger than the baseline value. There are four clear brightening events seen in the Juno-UVS data, and these are described in more detail below. It is noteworthy from Figure 3 that during the 8 days previous to the fourth event, there was a general increase in the total emitted power from the northern aurora of  $\sim 2$ –3 TW which coincided with a general increase in the solar wind ram pressure of 0.01–0.1 nPa. Comparing the emitted northern auroral power and the solar wind ram pressure data, there is a poor correlation ( $R = 0.22$ ) during the first half of the observations (3–13 June 2016), during which the first three brightening events occur, but a better correlation ( $R = 0.43$ ) in the second half of the observations (14–24 June 2016), during which the final brightening event occurs. Interestingly, the correlation between the total emitted power from the northern and southern auroras over the entire data set is quite high ( $R = 0.78$ ) but was much higher during the first half of the observations ( $R = 0.87$ ) than during the second half ( $R = 0.79$ ). This may be a result of the different nature of the aurora, as indicated by the changing correlation with the solar wind, but could also be due to the poorer and poorer view of the southern aurora as the sub-Juno latitude increases.

Figure 4 shows the time dependence of the total emitted northern auroral power during the four largest brightening events, which occurred near 5 June 2016 at 19:34 UT, 9 June 2016 at 13:34 UT, 11 June 2016 at 04:34 UT, and 21 June 2016 at 15:34 UT. The four event profiles have been scaled to a common peak brightness of 12 TW and shifted in time so that the peak brightness occurred in the first hour of relative time, in order to compare their time dependences. It is notable that all four events were closely grouped in central meridian longitude (CML), in the range of  $264^\circ$ – $296^\circ$ . This is considerably larger than the CML  $\sim 150^\circ$ – $210^\circ$  range where the northern aurora is most easily viewed [e.g., Connerney et al., 1996; Nichols et al., 2009], so that this phenomenon is not likely an artifact of auroral visibility. The first three brightening events were uncorrelated with solar wind variations (although it may be noteworthy that they occurred when the solar wind ram pressure was less than 0.1 nPa) and may be connected with the sudden release of plasma down Jupiter's magnetotail, as might be expected to occur during rotationally driven reconnection [e.g., Cowley et al., 2007; Kronberg et al., 2008; Louarn et al., 2015; Delamere et al., 2015; Walker and Jia, 2016], since they appear to have similar occurrence rates (every 2–4 days, when active). The time evolution of these three events is similar and is fairly well represented by exponentials with a  $1/e$  risetime of  $\sim 2$  h and a  $1/e$  decay time of  $\sim 5$  h. These events appear to be similar in all respects to those seen earlier with the Hisaki spacecraft [Kimura et al., 2015]. By contrast, the fourth brightening event, which correlates very well with a strong peak in the solar wind ram pressure (and which is identified as a likely corotating interaction region (R. Ebert, personal communication, 2017)), has a much different time evolution, with a much slower rise ( $\sim 5$  h) and more erratic decay.

#### 4. Conclusions

The arrival of the Juno spacecraft at Jupiter provided an excellent opportunity to investigate the relationship between local solar wind conditions and the Jovian aurora. The results from Juno-UVS indicate that, as perhaps expected for Jupiter's rotationally dominated magnetosphere, Jovian auroras are occasionally correlated with solar wind variations, but more often are not. These data presented an interesting and perhaps systematic variation of color ratio, with the largest color ratios (and thus most energetic precipitating particles) seen near the equatorward and nightside boundaries of the auroral region. While this color ratio gradient is most notable near the epochs of brightening events, it is present at quieter times as well. As the Juno mission proceeds, the focus of the polar magnetospheric science will turn to more detailed and high-resolution studies of specific auroral features and/or events. However, given the highly variable nature of auroral phenomena, it is still possible to learn important facts from low-resolution, synoptic observations; such data will be collected by Juno-UVS from the apojove regions of the Juno orbit as often as possible during the remainder of the mission.

#### Acknowledgments

We are grateful to NASA and contributing institutions which have made the Juno mission possible. This work was funded by NASA's New Frontiers Program for Juno via contract with the Southwest Research Institute. J.-C.G., D.C.G., and B.B. were supported by the PRODEX program managed by ESA in collaboration with the Belgian Federal Science Policy Office. The data presented here reside (May 2017) in the atmospheres node of NASA's Planetary Data System.

#### References

- Ajello, J. M., D. E. Shemansky, W. R. Pryor, A. I. F. Stewart, K. E. Simmons, T. Majeed, J. H. Waite Jr., G. R. Gladstone, and D. Grodent (2001), Spectroscopic evidence for high-altitude aurora at Jupiter from Galileo extreme ultraviolet spectrometer and Hopkins ultraviolet telescope observations, *Icarus*, *152*, 151.
- Badman, S. V., G. Branduardi-Raymont, M. Galand, S. L. G. Hess, N. Krupp, L. Lamy, H. Melin, and C. Tao (2015), Auroral processes at the giant planets: Energy deposition, emission mechanisms, morphology and spectra, *Space Sci. Rev.*, *187*, 99.
- Bagenal, F., et al. (2014), Magnetospheric science objectives of the Juno mission, *Space Sci. Rev.*, *1*, 69, doi:10.1007/s11214-014-0036-8.
- Bhardwaj, A., and G. R. Gladstone (2000), Auroral emissions of the giant planets, *Rev. Geophys.*, *38*, 295.
- Bonfond, B., et al. (2017), Morphology of the UV aurorae Jupiter during Juno's first perijove observations, *Geophys. Res. Lett.*, *44*, 4463–4471, doi:10.1002/2017GL073114.
- Broadfoot, A. L., et al. (1979), Extreme ultraviolet observations from Voyager 1: Encounter with Jupiter, *Science*, *204*, 979.
- Clarke, J. T., D. Grodent, S. W. H. Cowley, E. J. Bunce, P. Zarka, J. E. P. Connerney, and T. Satoh (2004), Jupiter's aurora, in *Jupiter: The Planet, Satellites and Magnetosphere*, edited by F. Bagenal, T. Dowling, and W. McKinnon, pp. 639–670, Cambridge Univ. Press, Cambridge, U. K.
- Clarke, J. T., et al. (2009), Response of Jupiter's and Saturn's auroral activity to the solar wind, *J. Geophys. Res.*, *114*, A05210, doi:10.1029/2008JA013694.
- Connerney, J. E. P., T. Satoh, and R. L. Baron (1996), Interpretation of auroral "lightcurves" with application to Jovian H<sub>3</sub><sup>+</sup> emissions, *Icarus*, *122*, 24–35.
- Connerney, J. E. P., et al. (2017), Jupiter's magnetosphere and aurorae observed by the Juno spacecraft during its first polar orbits, *Science*, doi:10.1126/science.aam5928.
- Cowley, S. W. H., J. D. Nichols, and D. J. Andrews (2007), Modulation of Jupiter's plasma flow, polar currents, and auroral precipitation by solar wind-induced compressions and expansions of the magnetosphere: A simple theoretical model, *Ann. Geophys.*, *25*, 1433–1463, doi:10.5194/angeo-25-1433-2007.
- Delamere, P. A., F. Bagenal, C. Paranicas, A. Masters, A. Radioti, B. Bonfond, L. Ray, X. Jia, J. Nichols, and C. Arridge (2015), Solar wind and internally driven dynamics: Influences on magnetodiscs and auroral responses, *Space Sci. Rev.*, *187*, 51–97, doi:10.1007/s11214-014-0075-1.
- Gérard, J.-C., B. Bonfond, D. C. Grodent, A. Radioti, J. T. Clarke, G. R. Gladstone, J. H. Waite Jr., D. Bisikalo, and V. I. Shematovich (2014), Mapping the electron energy in Jupiter's aurora: Hubble spectral observations, *J. Geophys. Res. Space Physics*, *119*, 9072–9088, doi:10.1002/2014J020514.
- Gladstone, G. R., et al. (2014), The ultraviolet spectrograph on NASA's Juno mission, *Space Sci. Rev.*, *1*–27, doi:10.1007/s11214-014-0040-z.
- Greathouse, T. K., G. R. Gladstone, M. W. Davis, D. C. Slater, M. H. Versteeg, K. B. Persson, B. C. Walther, G. S. Winters, S. C. Persyn, and J. S. Eterno (2013), Performance results from in-flight commissioning of the Juno ultraviolet spectrograph (Juno-UVS), *Proc. SPIE*, *8859*, 88590T.
- Grodent, D. C. (2015), A brief review of ultraviolet auroral emissions on giant planets, *Space Sci. Rev.*, *187*, 23–50, doi:10.1007/s11214-014-0052-8.
- Gurnett, D. A., et al. (2002), Control of Jupiter's radio emission and aurorae by the solar wind, *Nature*, *415*, 985–987.
- Gustin, J., D. C. Grodent, L. C. Ray, B. Bonfond, E. J. Bunce, J. D. Nichols, and N. Ozak (2016), Characteristics of north Jovian aurora from STIS FUV spectral images, *Icarus*, *268*, 215–241, doi:10.1016/j.icarus.2015.12.048.
- Kimura, T., et al. (2015), Transient internally driven aurora at Jupiter discovered by Hisaki and the Hubble Space Telescope, *Geophys. Res. Lett.*, *42*, 1662–1668, doi:10.1002/2015GL063272.
- Kimura, T., et al. (2016), Jupiter's X-ray and EUV auroras monitored by Chandra, XMM-Newton, and Hisaki satellite, *J. Geophys. Res. Space Physics*, *121*, 2308–2320, doi:10.1002/2015JA021893.
- Kita, H., et al. (2016), Characteristics of solar wind control on Jovian UV auroral activity deciphered by long-term Hisaki EXCEED observations: Evidence of preconditioning of the magnetosphere?, *Geophys. Res. Lett.*, *43*, 6790–6798, doi:10.1002/2016GL069481.
- Kronberg, E. A., J. Woch, N. Krupp, A. Lagg, P. W. Daly, and A. Korth (2008), Comparison of periodic substorms at Jupiter and Earth, *J. Geophys. Res.*, *113*, A04212, doi:10.1029/2007JA012880.
- Louarn, P., N. Andre, C. M. Jackman, S. Kasahara, E. A. Kronberg, and M. F. Vogt (2015), Magnetic reconnection and associated transient phenomena within the magnetospheres of Jupiter and Saturn, *Space Sci. Rev.*, *187*, 181–227, doi:10.1007/s11214-014-0047-5.
- McComas, D. J., et al. (2013), The Jovian Auroral Distributions Experiment (JADE) on the Juno mission to Jupiter, *Space Sci. Rev.*, *1*–97, doi:10.1007/s11214-013-9990-9.
- Nichols, J. D., J. T. Clarke, J.-C. Gérard, D. C. Grodent, and K. C. Hansen (2009), Variation of different components of Jupiter's auroral emission, *J. Geophys. Res.*, *114*, A06210, doi:10.1029/2009JA014051.
- Nichols, J. D., et al. (2017), Response of Jupiter's auroras to conditions in the interplanetary medium as measured by the Hubble Space Telescope and Juno, *Geophys. Res. Lett.*, doi:10.1002/2017GL073029, in press.

- Prangé, R., D. Rego, D. Southwood, P. Zarka, S. Miller, and W.-H. Ip (1996), Rapid energy dissipation and variability of the Io-Jupiter electrodynamic circuit, *Nature*, *379*, 323.
- Pryor, W. R., et al. (2005), Cassini UVIS observations of Jupiter's auroral variability, *Icarus*, *178*, 312–326.
- Tao, C., et al. (2015a), Variation of Jupiter's aurora observed by Hisaki/EXCEED: 1. Observed characteristics of the auroral electron energies compared with observations performed using HST/STIS, *J. Geophys. Res. Space Physics*, *121*, 4041–4054, doi:10.1002/2015JA021271.
- Tao, C., T. Kimura, S. V. Badman, N. André, F. Tsuchiya, G. Murakami, K. Yoshioka, I. Yoshikawa, A. Yamazaki, and M. Fujimoto (2015b), Variation of Jupiter's aurora observed by Hisaki/EXCEED: 2. Estimations of auroral parameters and magnetospheric dynamics, *J. Geophys. Res. Space Physics*, *121*, 4055–4071, doi:10.1002/2015JA021272.
- Walker, R. J., and X. Jia (2016), Simulation studies of plasma transport at Earth, Jupiter, and Saturn, in *Magnetic Reconnection, Astrophys. Space Sci. Library*, vol. 427, edited by W. Gonzalez and E. Parker, pp. 345–372, Springer Int. Publ., Basel, Switzerland.
- Yung, Y. L., G. R. Gladstone, K. M. Chang, J. M. Ajello, and S. K. Srivastava (1982), H<sub>2</sub> fluorescence spectrum from 1200 to 1700 Å by electron impact—Laboratory study and application to Jovian aurora, *Astrophys. J.*, *254*, L65–L69.